Article

Secondary ice formation in idealised deep convection: Source of primary ice and impact on glaciation – Supplementary Information

Annette K. Miltenberger [1,*], Tim Lüttmer [1] and Christoph Siewert [2]

[1] Institute for Atmospheric Physics, Johannes Gutenberg University Mainz, Germany
[2] Deutscher Wetterdienst, Offenbach, Germany

Version May 22, 2020 submitted to Atmosphere

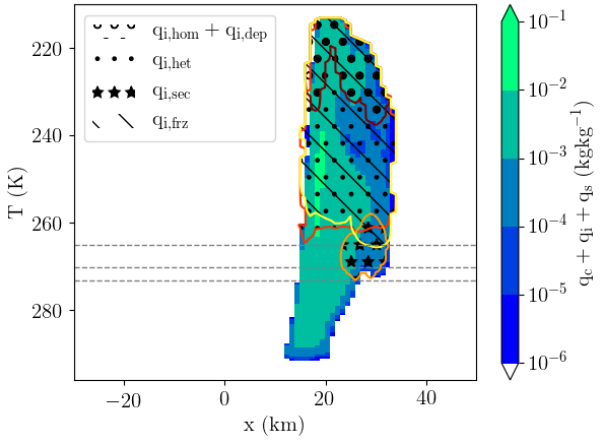

Figure S1. Cross-section through the deep convective cloud 30 min after the start of the simulation with a wind shear of 25 m s^{-1} (at y = 0 km). The colour shading shows the mass mixing ratio of cloud droplets, ice (all modes) and snow. Different hatching indicates areas with mass mixing ratios of the different ice modes (see legend) in excess of 1 mg kg^{-1}. The data has been regridded to a regular temperature grid using the model air temperature. The grey dashed lines highlight temperatures of 0 °C, −3 °C, and −5 °C.

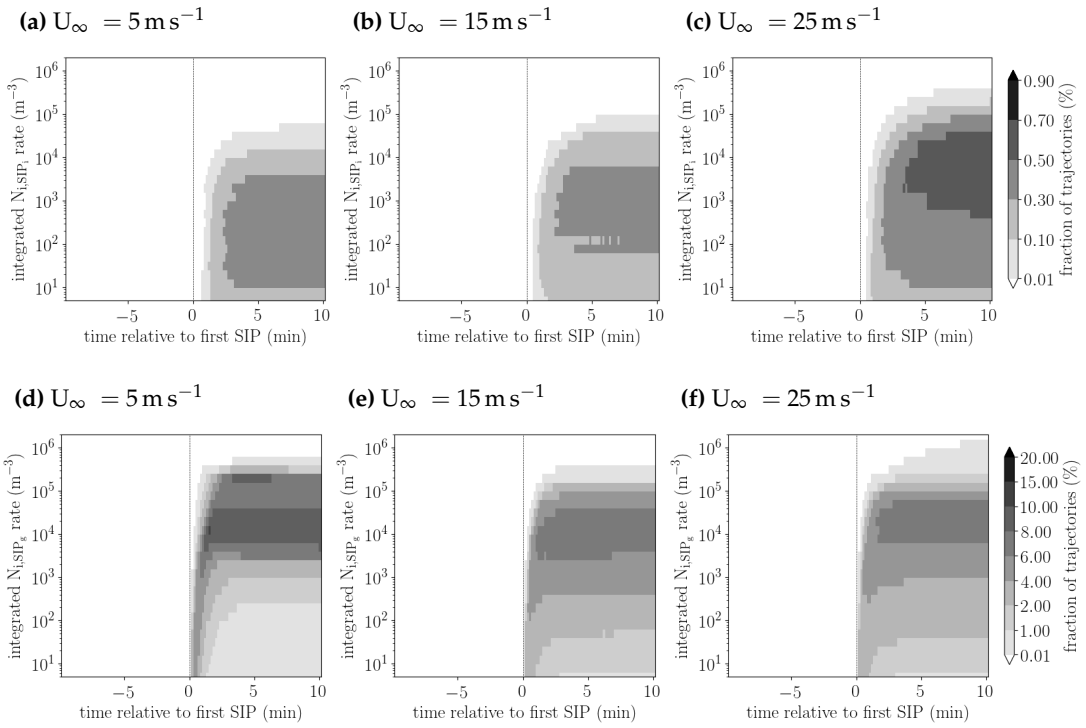

Figure S2. Composite evolution of integrated ice crystal number concentration rates due to SIP on riming ice crystals and snow **(a-c)** and due to SIP on riming graupel **(d-f)**. Note the different color scales in the two rows. Composites are centred on the time of the first SIP event along each trajectory. In the shown simulations heterogeneous freezing commences at $-5\,°C$.

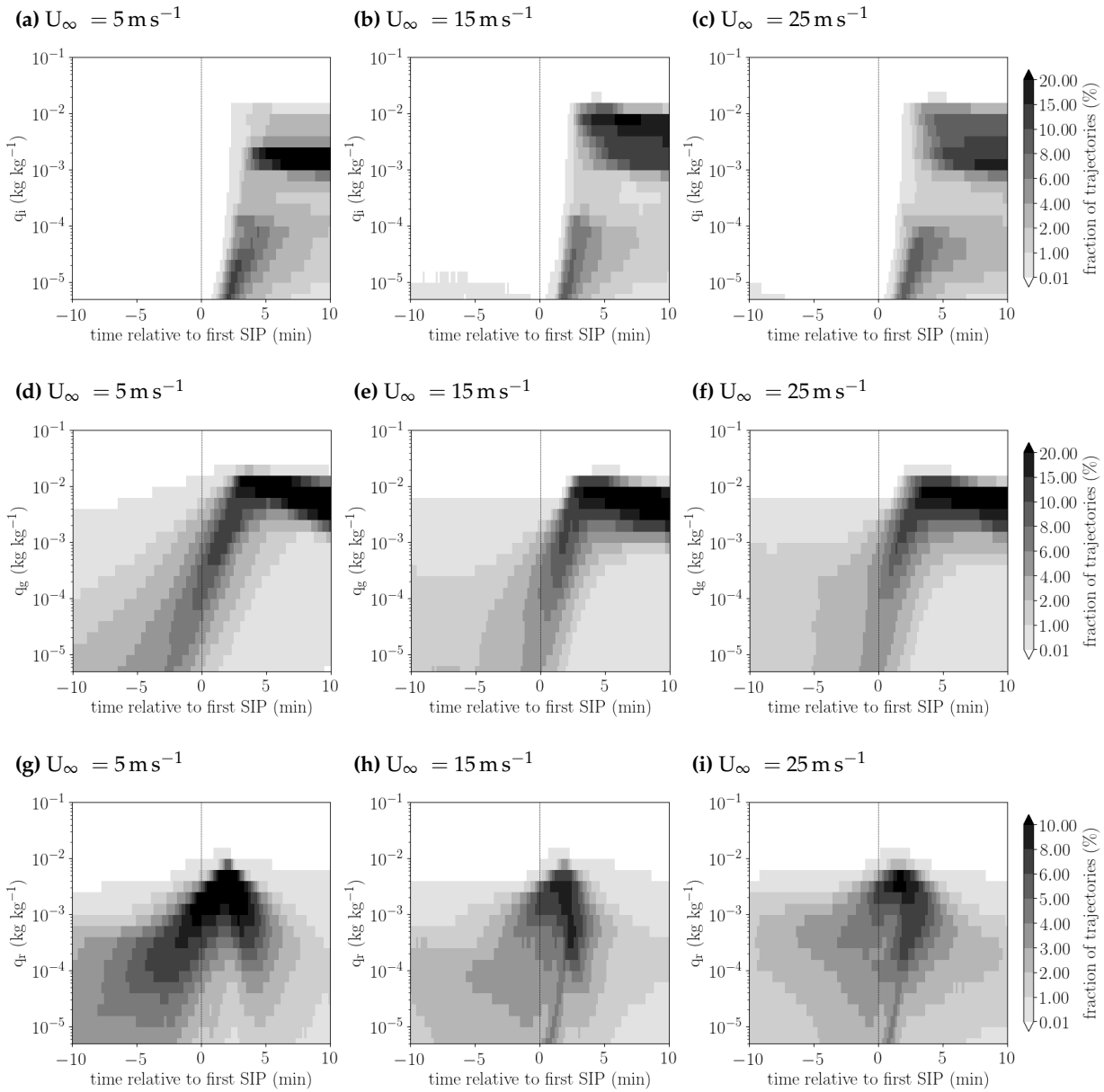

Figure S3. Composite evolution of mass mixing ratios of ice crystals (a-c), graupel (d-f) and rain drops (g-i) along trajectories relative to the time and altitude of the first SIP event for simulations with $U_\infty = 5\,m\,s^{-1}$ (a, d, g), $15\,m\,s^{-1}$ (b, e, h) and $25\,m\,s^{-1}$ (c, f, i). In the shown simulations heterogeneous freezing commences at $-5\,°C$.

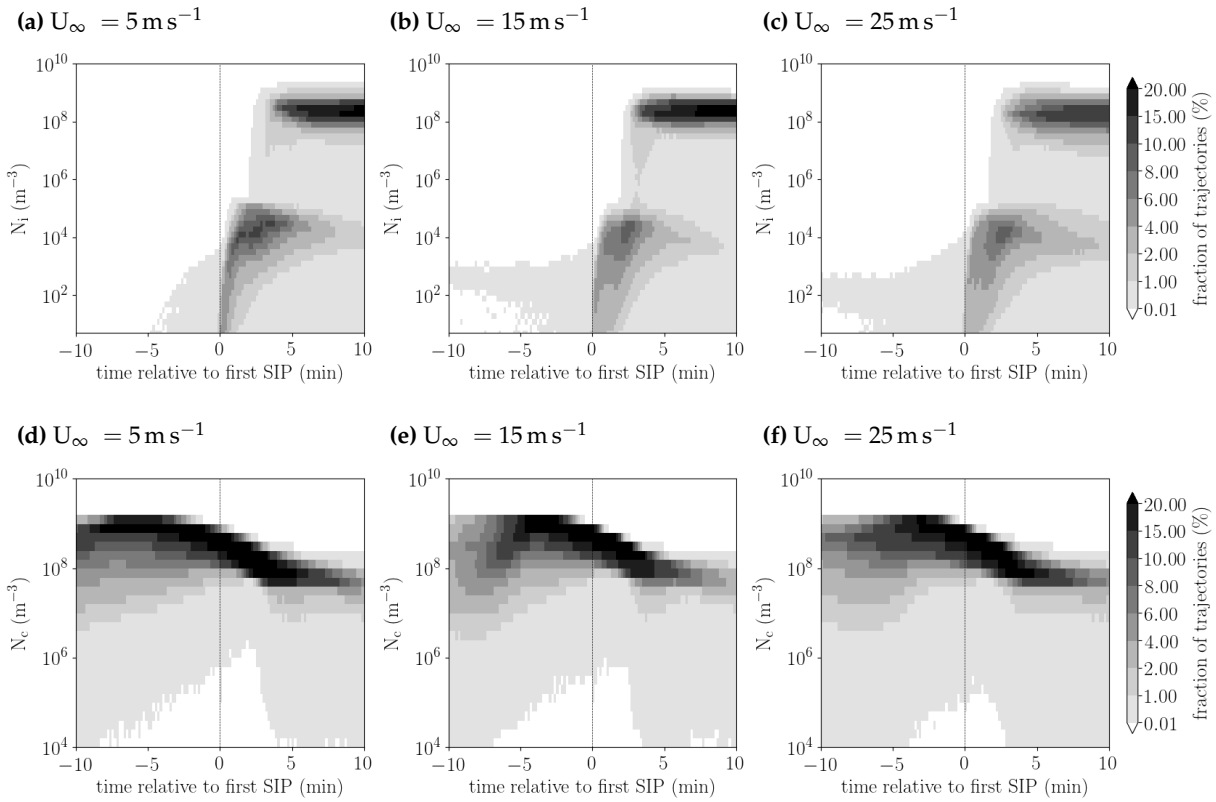

Figure S4. Composite evolution of number concentrations of ice crystals (**a-c**), and cloud droplets (**d-f**) along trajectories relative to the time and altitude of the first SIP event for simulations with $U_\infty = 5\,m\,s^{-1}$ (a, d), $15\,m\,s^{-1}$ (**b, e**) and $25\,m\,s^{-1}$ (**c, f**). In the shown simulations heterogeneous freezing commences at $-5\,°C$.

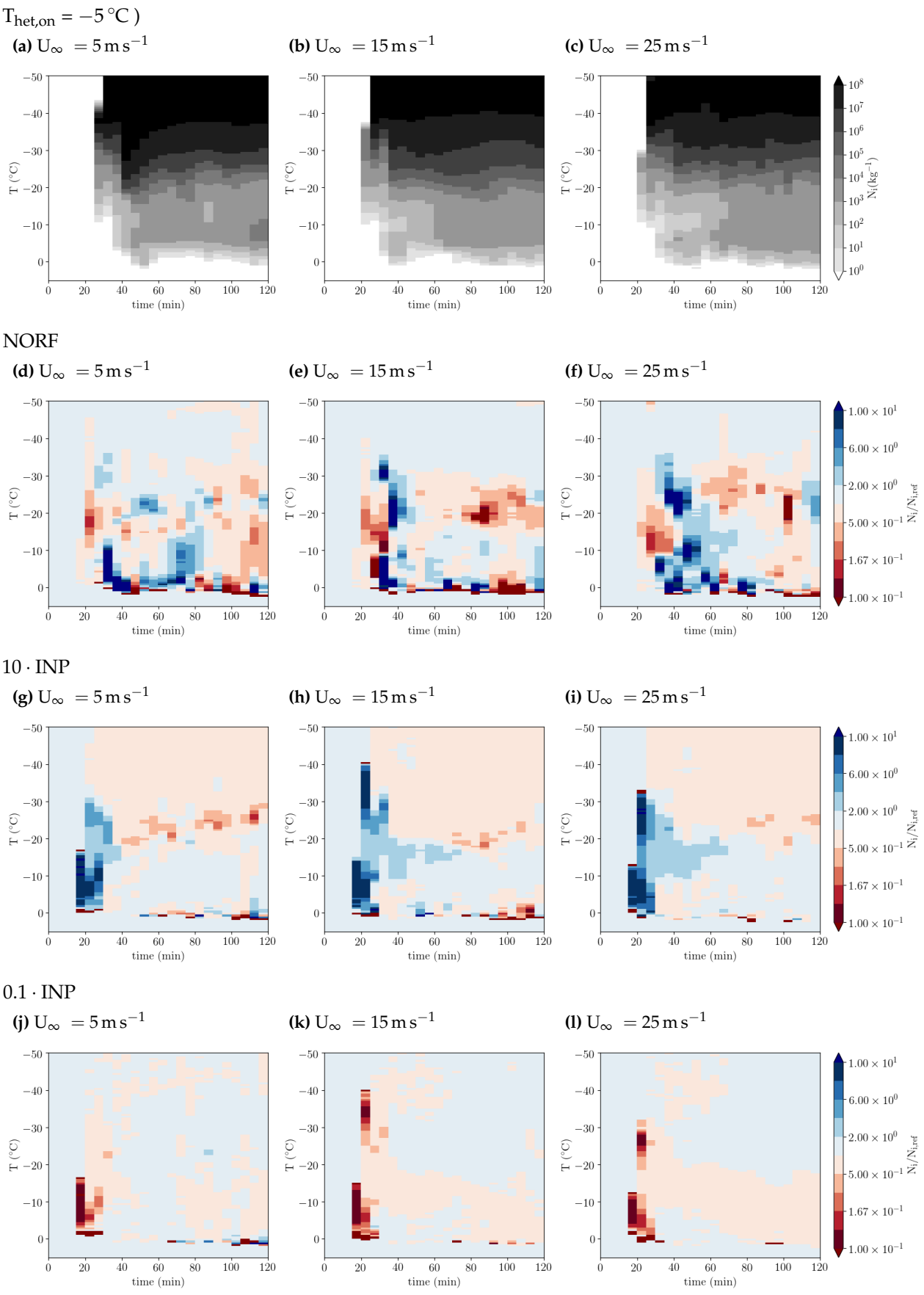

Figure S5. **(a-c)** Average number concentration of ice crystals in the reference simulation ($T_{het,on}$ = −5 °C) as a function of simulation time and air temperature (shading). **(d-l)** Change of the average number concentration of ice crystals relative to the reference simulations. The different columns shows simulations with different vertical wind shear and different rows the various sensitivity experiments.

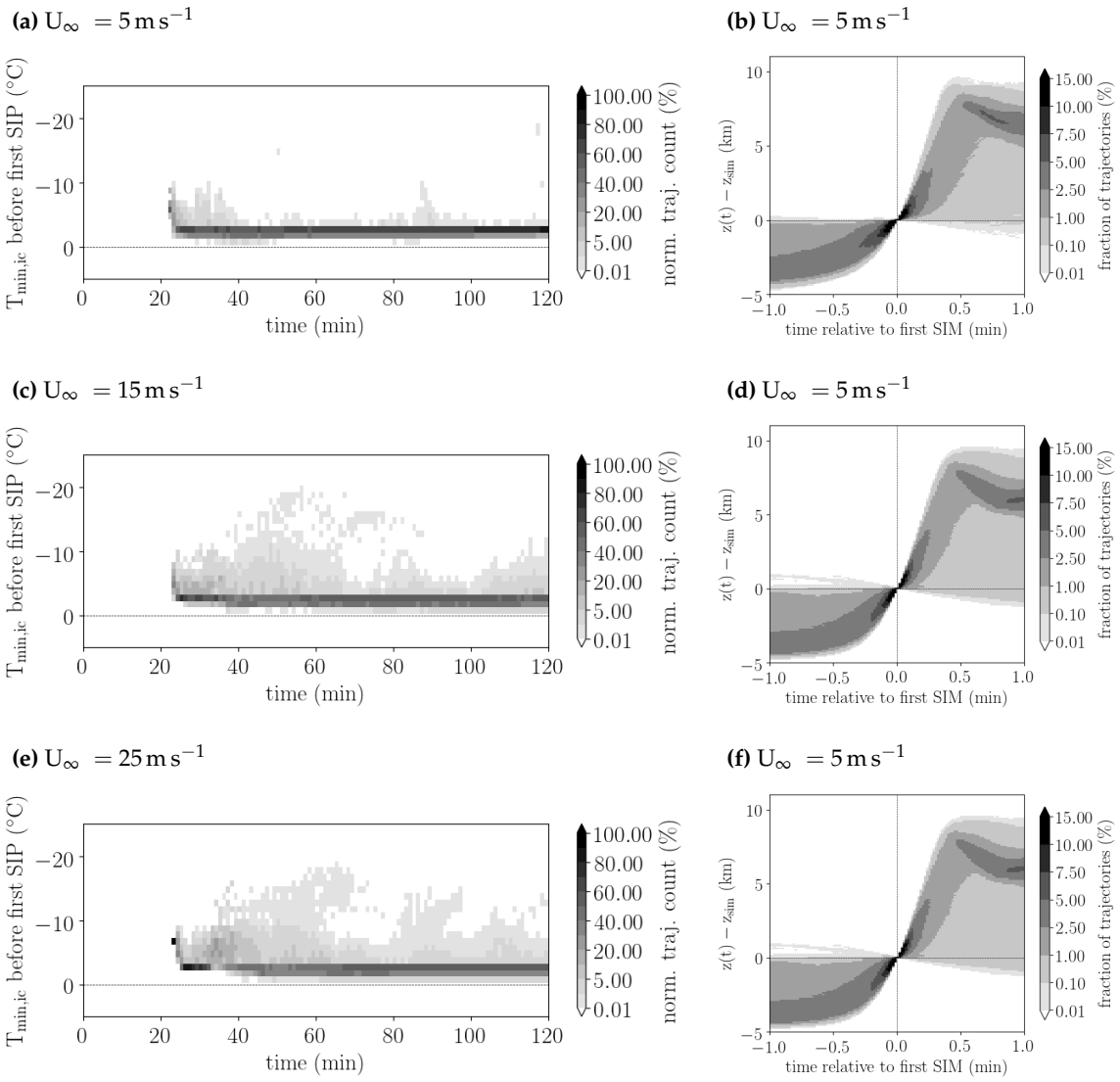

Figure S6. (**a, c, e**) Distribution of minimum temperatures along trajectories in 10 min prior to first SIP event in simulations with $T_{het,on} = -10\,^\circ$°C. The shading indicates the frequency of occurrence of a particular minimum temperature, the ordinate corresponds to the simulation time, at which the SIP event occurred. (**b, d, f**) Composite evolution of trajectory altitude relative to the time and altitude of the first SIP event in simulations with $T_{het,on} = -10\,^\circ$°C. The different rows shows simulations with different vertical wind shear: (**a, b**) $U_\infty = 5\,m\,s^{-1}$, (**c, d**) $15\,m\,s^{-1}$, and (**e, f**) $25\,m\,s^{-1}$.

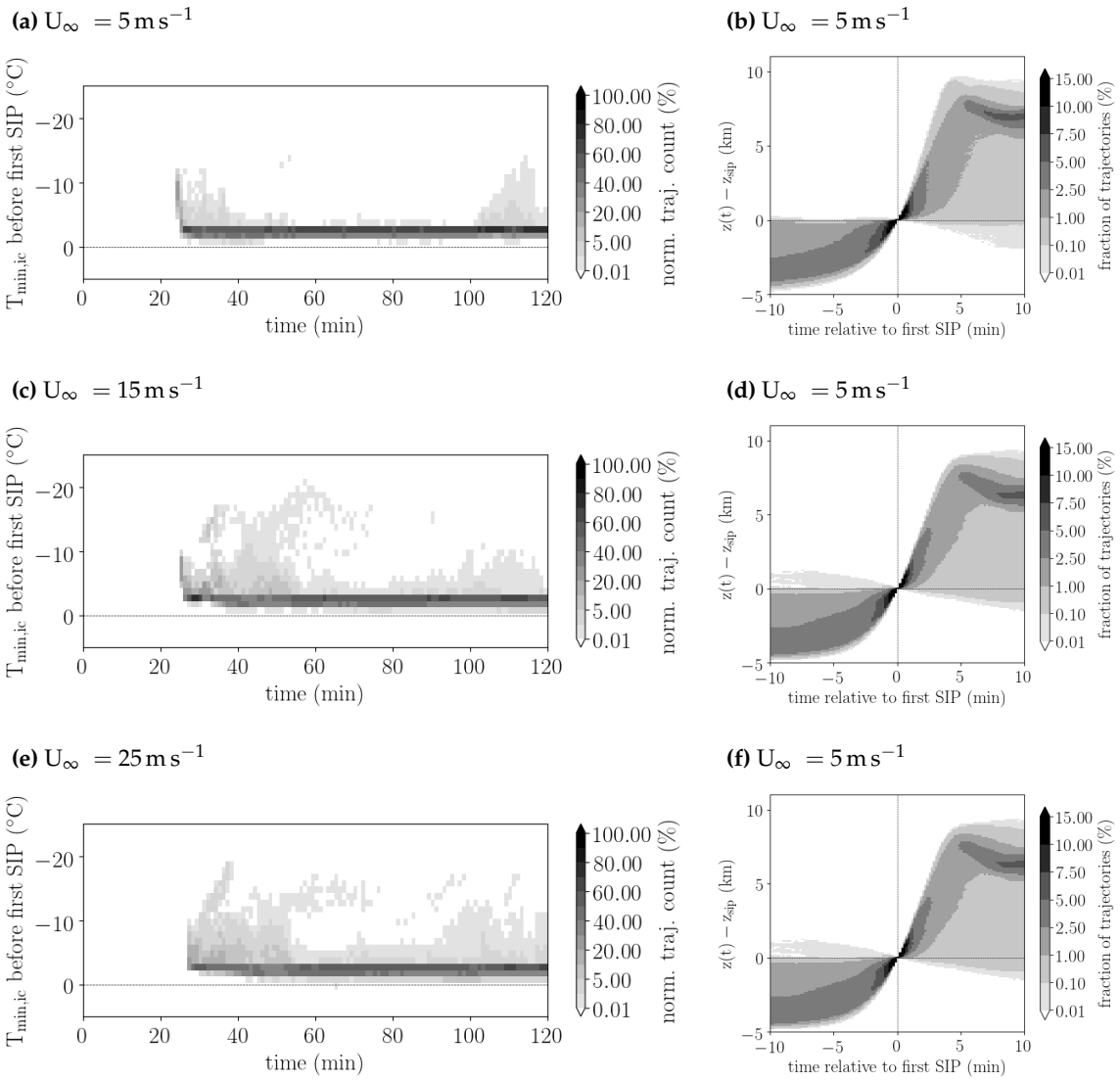

Figure S7. (**a, c, e**) Distribution of minimum temperatures along trajectories in 10 min prior to first SIP event in simulations without a rain freezing parameterisation. The shading indicates the frequency of occurrence of a particular minimum temperature, the ordinate corresponds to the simulation time, at which the SIP event occurred. (**b, d, f**) Composite evolution of trajectory altitude relative to the time and altitude of the first SIP event in simulations without a rain freezing parameterisation. The different rows shows simulations with different vertical wind shear: (**a, b**) $U_\infty = 5\,m\,s^{-1}$, (**c, d**) $15\,m\,s^{-1}$, and (**e, f**) $25\,m\,s^{-1}$. In the shown simulations heterogeneous freezing commences at $-5\,°C$.

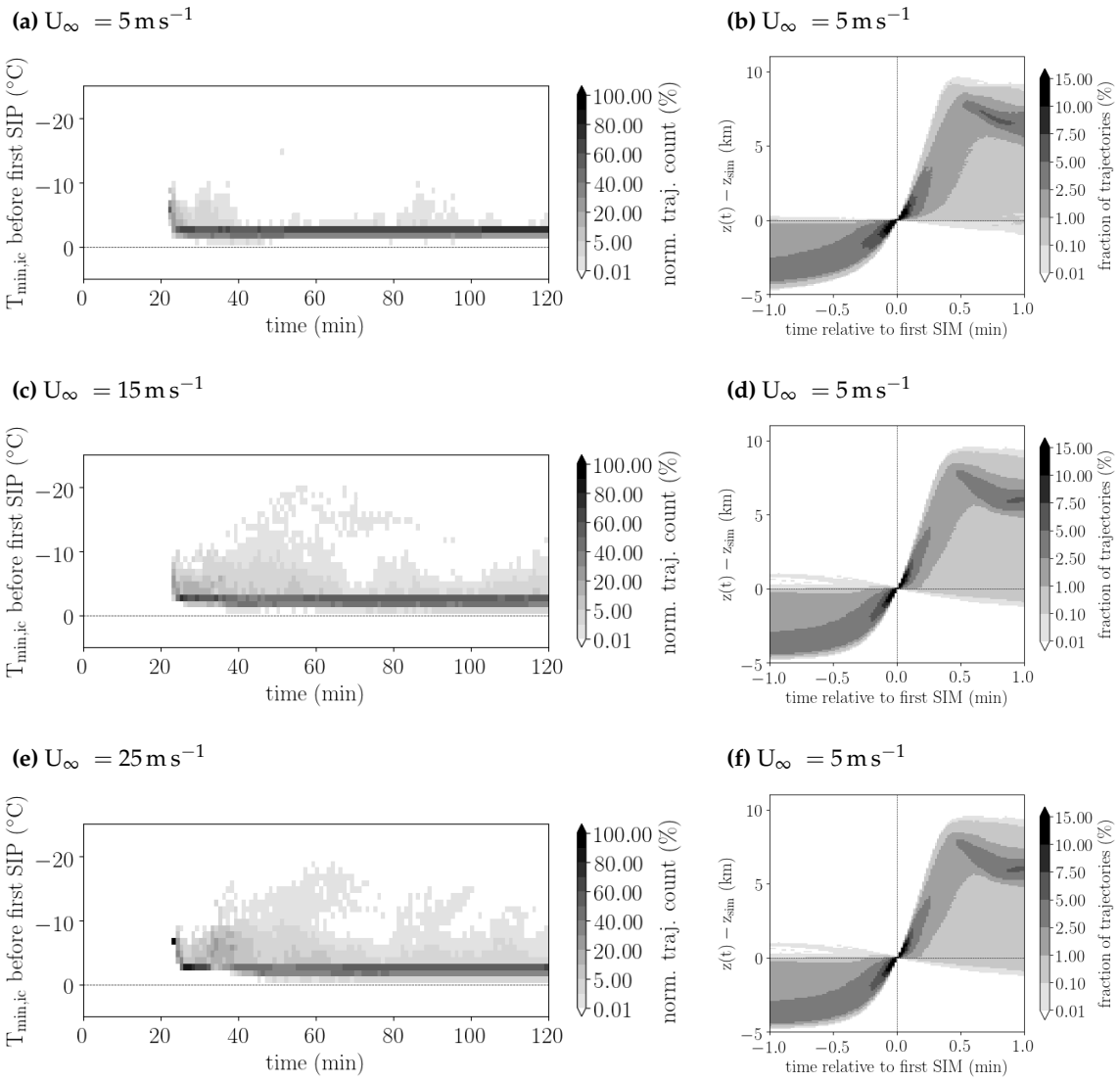

Figure S8. (**a, c, e**) Distribution of minimum temperatures along trajectories in 10 min prior to first SIP event in simulations with a factor 10 larger INP concentrations than in the reference simulation. The shading indicates the frequency of occurrence of a particular minimum temperature, the ordinate corresponds to the simulation time, at which the SIP event occurred. (**b, d, f**) Composite evolution of trajectory altitude relative to the time and altitude of the first SIP event in simulations without a rain freezing parameterisation. The different rows shows simulations with different vertical wind shear: (**a, b**) $U_\infty = 5\,m\,s^{-1}$, (**c, d**) $15\,m\,s^{-1}$, and (**e, f**) $25\,m\,s^{-1}$. In the shown simulations heterogeneous freezing commences at $-5\,°C$.

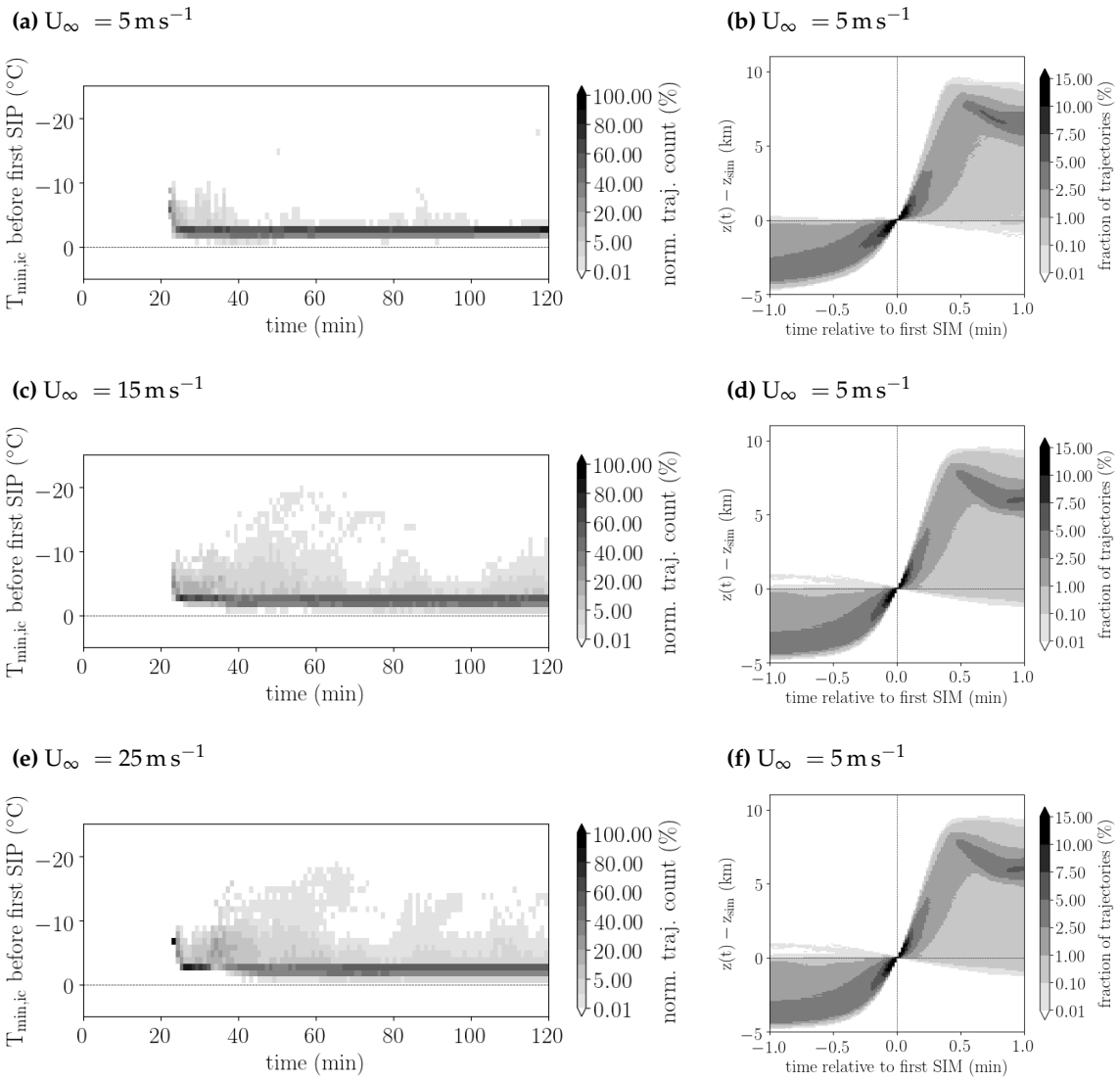

Figure S9. (**a, c, e**) Distribution of minimum temperatures along trajectories in 10 min prior to first SIP event in simulations with a factor 10 smaller INP concentrations than in the reference simulation. The shading indicates the frequency of occurrence of a particular minimum temperature, the ordinate corresponds to the simulation time, at which the SIP event occurred. (**b, d, f**) Composite evolution of trajectory altitude relative to the time and altitude of the first SIP event in simulations without a rain freezing parameterisation. The different rows shows simulations with different vertical wind shear: (**a, b**) $U_\infty = 5\,m\,s^{-1}$, (**c, d**) $15\,m\,s^{-1}$, and (**e, f**) $25\,m\,s^{-1}$. In the shown simulations heterogeneous freezing commences at $-5\,°C$.

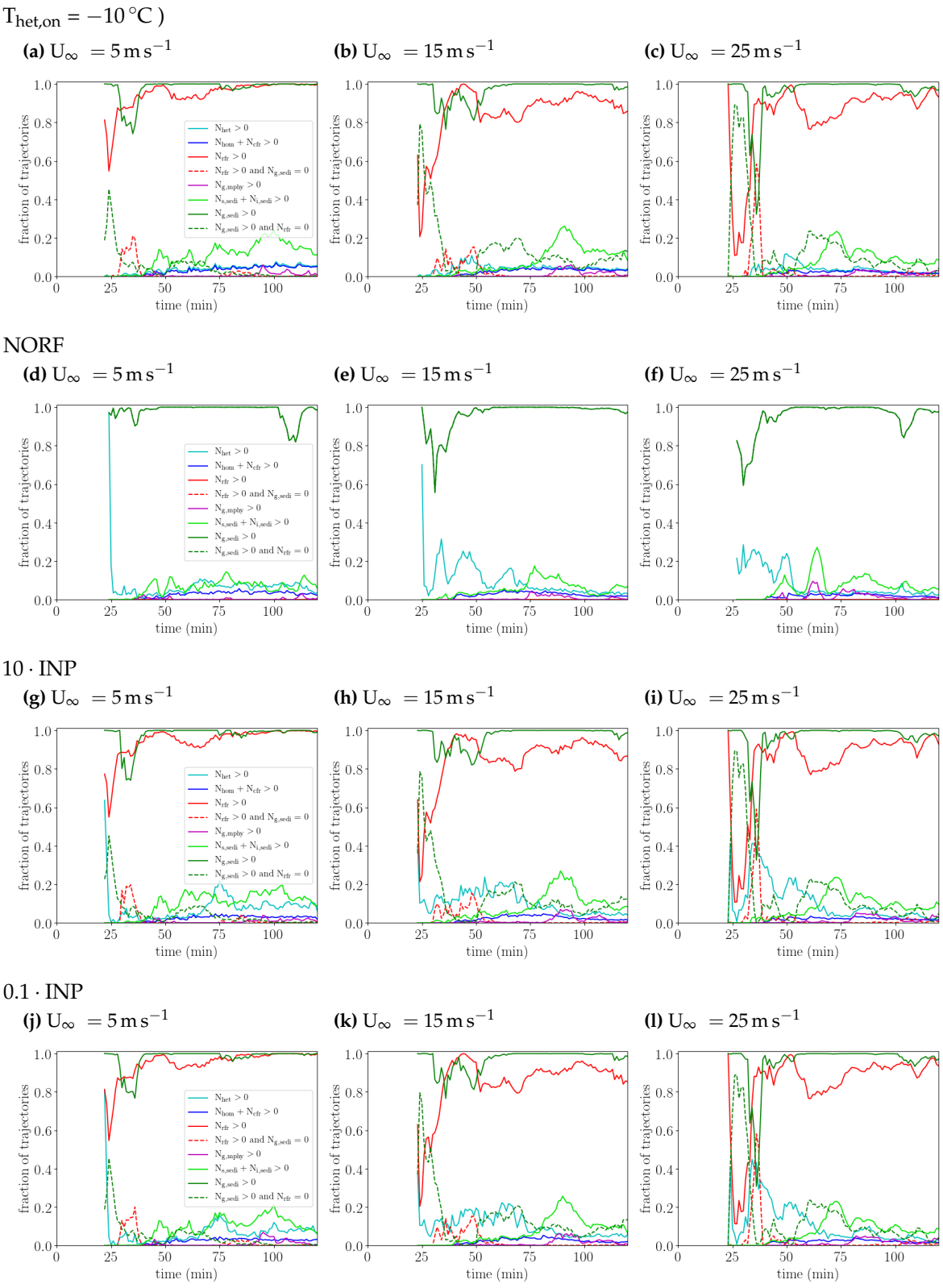

Figure S10. Fraction of trajectories, in which heterogeneous freezing (cyan), homogeneous freezing (blue), rain drop freezing (red), sedimentation influx of ice and snow (light green), graupel formation by deposition or riming, or sedimentation influx of graupel (dark green) happened during the 10 min before the first SIP event. The abscissa shows the time after the start of the simulation, at which the SIP event occurred. The red (dark green) dashed lines indicates the fraction of trajectories, which are not influenced by graupel sedimentation (rain freezing) but in which rain freezing (graupel sedimentation) occurs. The different columns shows simulations with different vertical wind shear and different rows the various sensitivity experiments.

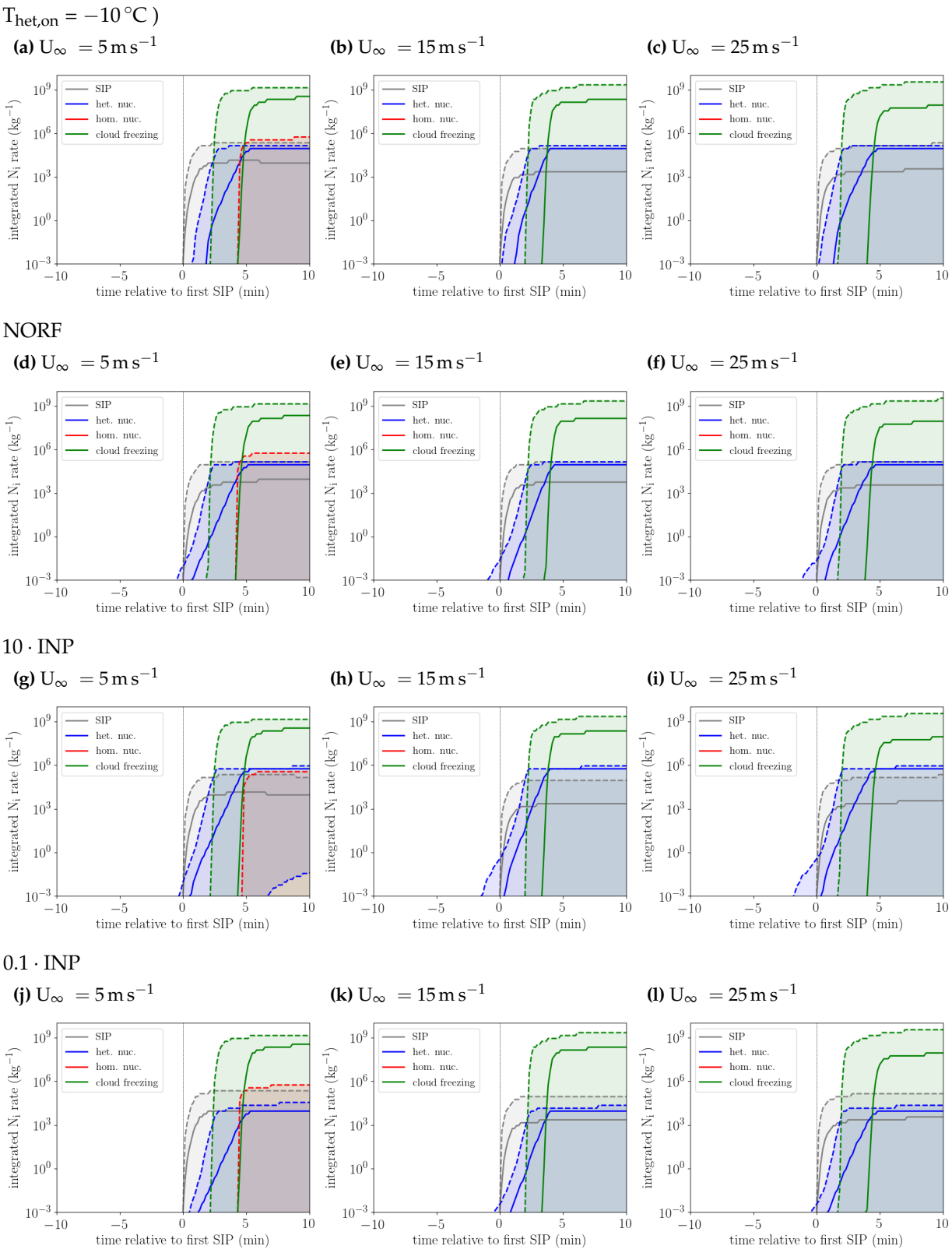

Figure S11. Composite evolution of integrated ice crystal number concentration rates due to SIP (grey), heterogeneous freezing (blue), homogeneous nucleation (cyan), and homogeneous cloud droplet freezing (green). Solid (dashed) lines show the 50th (99th and 1st) percentile of the rates from all trajectories. Composites are centred on the time of the first SIP event along each trajectory. The different columns shows simulations with different vertical wind shear and different rows the various sensitivity experiments.

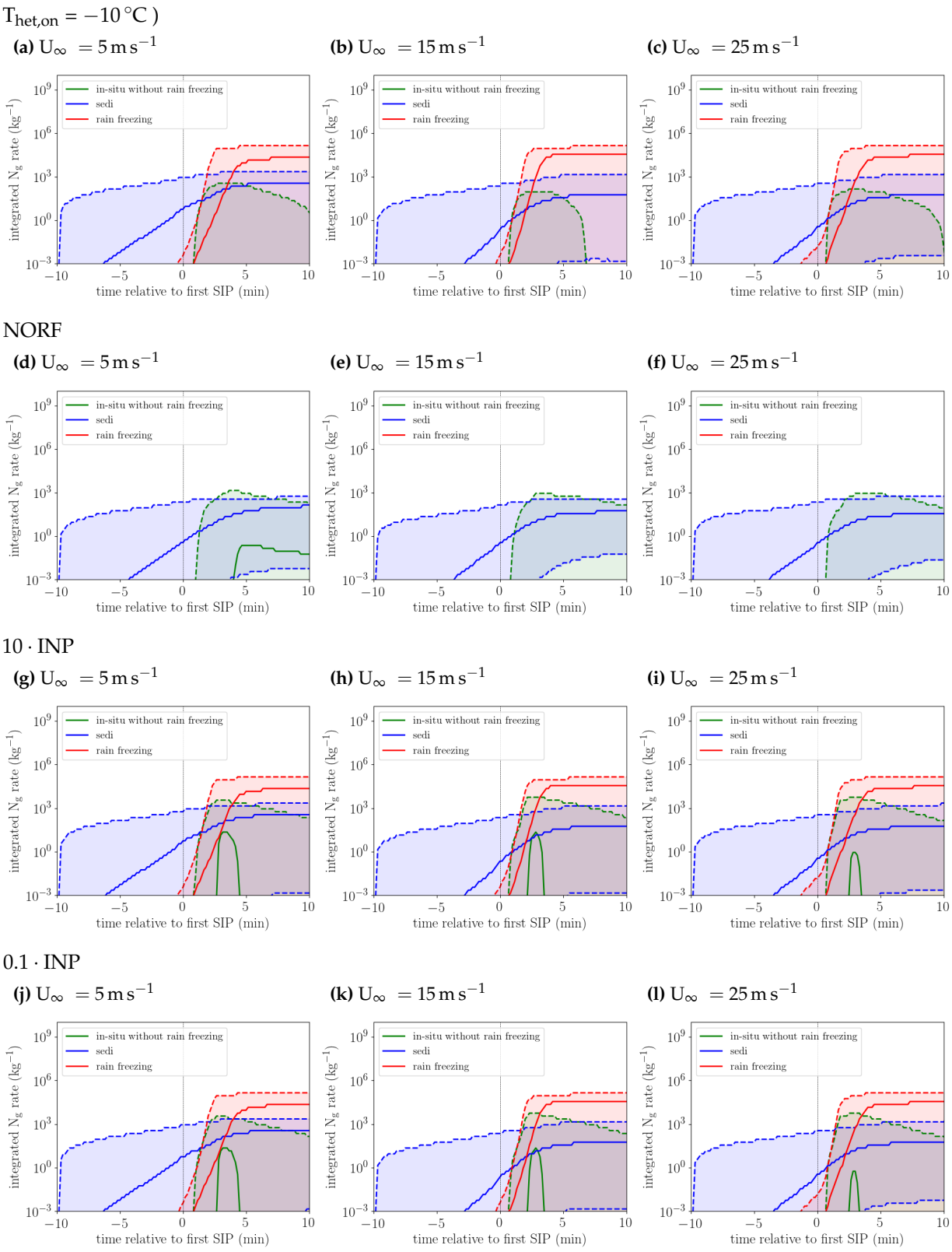

Figure S12. Composite evolution of integrated graupel number concentration rates due to riming (magenta), sedimentation influx (blue), and rain freezing (red). Solid (dashed) lines show the 50th (99th and 1st) percentile of the rates from all trajectories. Composites are centred on the time of the first SIP event along each trajectory. The different columns shows simulations with different vertical wind shear and different rows the various sensitivity experiments.

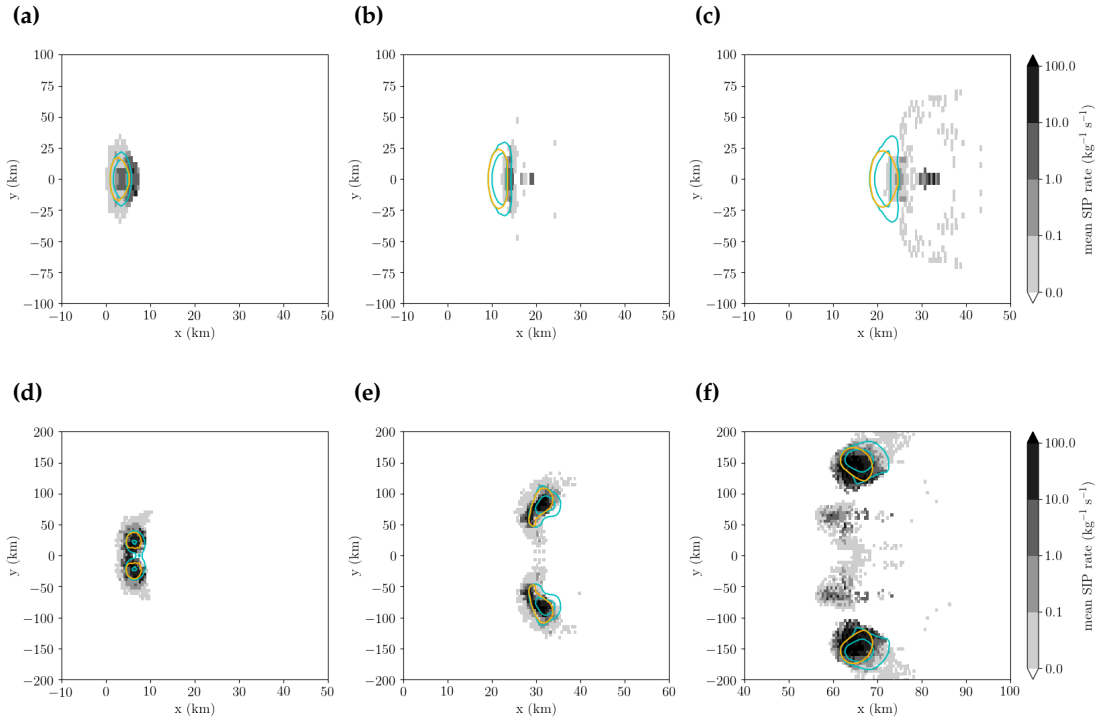

Figure S13. Updraft cores (cyan contours: $15\,\mathrm{m\,s^{-1}}$ and $30\,\mathrm{m\,s^{-1}}$) and average SIP rate (shading) at simulations times of 35 min (**a-c**) and 100 min (**d-f**). The orange contour encircles the region in the Hallett-Mossop zone with vertical velocities larger than $15\,\mathrm{m\,s^{-1}}$. The different columns shows simulations with different vertical wind shear: (**a, d**) $\mathrm{U}_\infty = 5\,\mathrm{m\,s^{-1}}$, (**b, e**) $15\,\mathrm{m\,s^{-1}}$, and (**c, f**) $25\,\mathrm{m\,s^{-1}}$. In the shown simulations heterogeneous freezing commences at $-5\,^\circ\mathrm{C}$ and no rain freezing parameterisation is used. Note different sections of the simulation domain are shown reflecting the varying propagation speed of the cells in different windshear conditions.

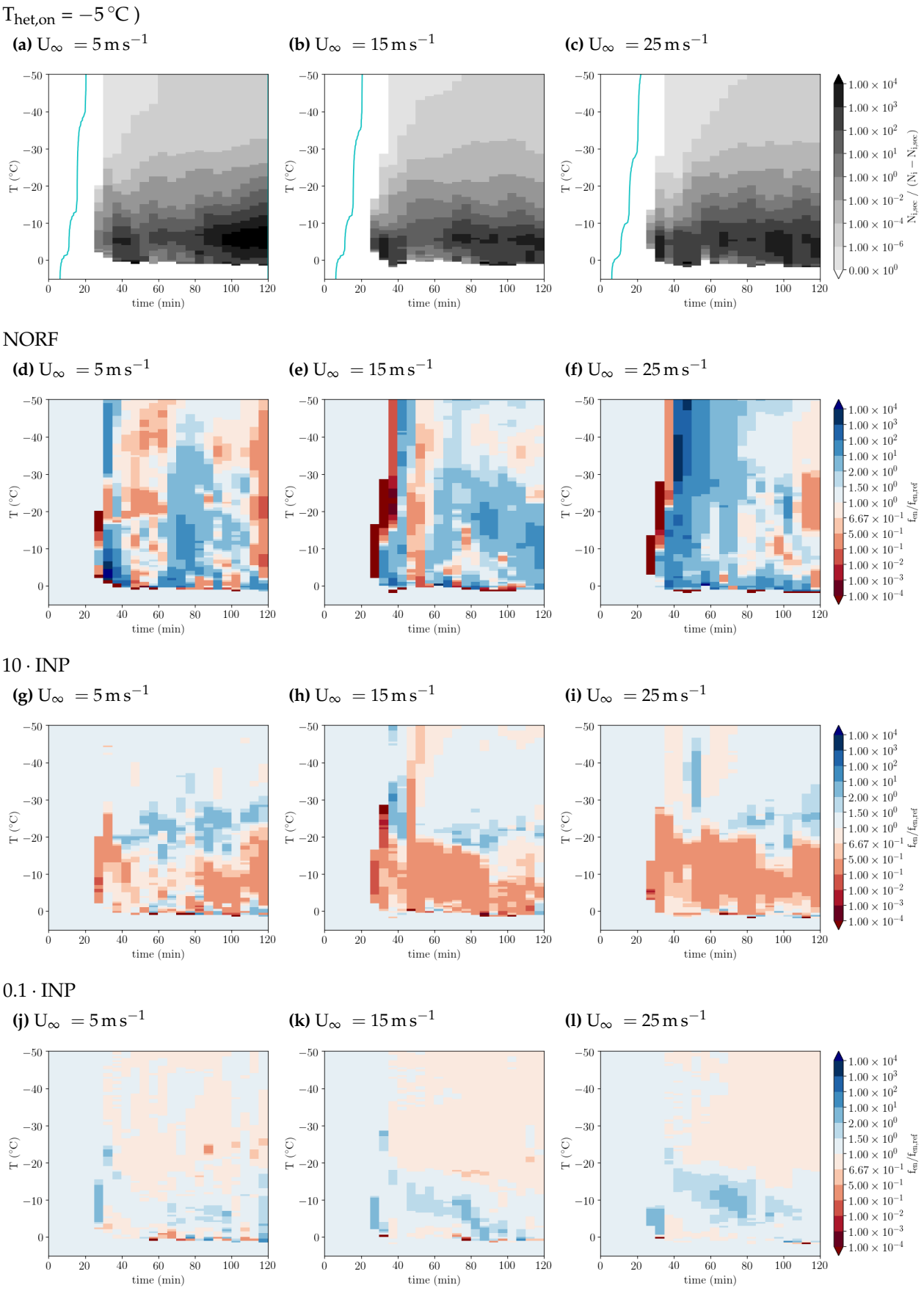

Figure S14. Change in the ratio of secondary ice number concentration to number concentration of primary ice crystals formed by other processes relative to the reference simulations ($T_{het,on} = -5\,°C$) as a function of simulation time and air temperature (shading). The upper row shows simulations with a parameterisation of rain freezing and the lower row ones without a rain freezing parameterisation. The cyan line indicates the onset of cloud fraction larger than 0.01. The different columns shows simulations with different vertical wind shear and different rows the various sensitivity experiments.